Synthesis of strontium iridates thin films by cathode sputtering: comparison with traditional laser ablation technology

© *Yu.V. Kislinskii* [1], *I.E. Moskal* [1], *A.M. Petrzhik* [1], *A.V. Shadrin* [1,2], *G.A. Ovsyannikov* [1]

[1] Kotelnikov Institute of Radio Engineering and Electronics of the RAS,
Moscow, Russia
[2] Moscow Institute of Physics and Technology (National Research University),
Dolgoprudny, Moscow Region, Russia

E-mail: yulii@hitech.cplire.ru

The technology of obtaining structured thin films of strontium iridates of the compositions $SrIrO_3$ and Sr_2IrO_4 by direct current cathode sputtering is presented. Both compositions were synthesized using the stoichiometric target Sr_2IrO_4, only the technological parameters varied. The composition of the resulting films was determined by the operating pressure and temperature. The electrophysical and structural properties of the obtained dielectric Sr_2IrO_4 and „metallic" $SrIrO_3$ films are discussed. The dielectric series is compared with Sr_2IrO_4 films obtained by laser ablation previously.

Keywords: strontium iridate, cathode sputtering, metals, disordered structures, hopping conductivity, activation energy of charge carriers.

1. Introduction

Strontium iridates with various chemical compositions belong to Ruddlesen-Proper series, where Sr_2IrO_4 — dielectric, $Sr_3Ir_2O_7$ — hopping conductor, $SrIrO_3$ — paramagnetic metal. Iridates feature strong spin-orbit interaction (up to 0.5 eV). In terms of crystal structure, Sr_2IrO_4 is similar to superconducting La_2CuO_4 and demonstrates antiferromagnetic properties at a temperature below 240 K. Synthesis of iridate thin films by the laser ablation and RF magnetron sputtering methods features the possibility of producing various phases and their mixture from a target with a fixed composition. Thus, for example, as many as several strontium iridate phases were produced from $SrIrO_3$ target: $SrIrO_3$, Sr_2IrO_4, $Sr_3Ir_2O_7$, depending on deposition conditions [1]. A similar experiment was also successfully performed for $Sr_3Ir_2O_7$ target [2]. Dielectric iridate is of interest as a material with strong spin-orbit interaction and antiferromagnetic ordering. Interesting features were experimentally recorded in Josephson heterostructure $Nb/Sr_2IrO_4/YBa_2Cu_3O_x$ with such iridate interlayer [3]. In all studies mentioned above, the laser ablation method was used for production of iridate thin films and heterostructures based on them. The objective of the study is to describe the growth process of strontium iridates $SrIrO_3$ and Sr_2IrO_4 by the DC cathode sputtering method (DC sputtering) and to define the structural and electrophysical parameters of the produced films.

2. Experimental

The thin films were synthesized by DC cathode sputtering of Sr_2IrO_4 target in pure argon on (110) $NdGaO_3$ substrates. The target was prepared from a mixture of $SrCO_3$ and IrO_2 powders using a standard ceramic process [4]. By variation of operating pressure of argon and substrate temperature, various strontium iridate phases were produced — $SrIrO_3$ and Sr_2IrO_4. Samples N 3 and 15 represent different strontium iridate phases produced from a single target by the DC cathode sputtering method. Film N 3 — metallic $SrIrO_3$ synthesized at 1.3 mBar and 770°C. The synthesis of dielectric Sr_2IrO_4 (film N 15) requires higher temperature 820°C and lower pressure 0.5 mBar. Figure 1 shows X-ray diffraction patterns for the two samples prepared by the DC cathode sputtering method and Sr_2IrO_4 sample synthesized by the laser ablation method (pulsed laser deposition or PLD), A3 PLD, is given for comparison.

Sample A3 was deposited using 2 Hz 1.6 J/cm² KrF excimer laser at Ar 0.5 mBar, $T = 800-760°C$. Its X-ray diffraction pattern is shown in Figure 1, *a*. Figure 1, *c* shows a secondary polycrystalline iridium phase. This phenomenon may be explained by suggesting that, when the deposition rate increases (by increasing power applied to the cathode), the iridium transfer rate increases faster than that of strontium. For producing sample N 15, deposition rate was reduced resulting in considerable reduction of the polycrystalline iridium fraction in the film as shown by comparison in Figure 1, *b* and *c*. Further $SrIrO_3$ samples deposited at a lower rate did not contain the iridium phase
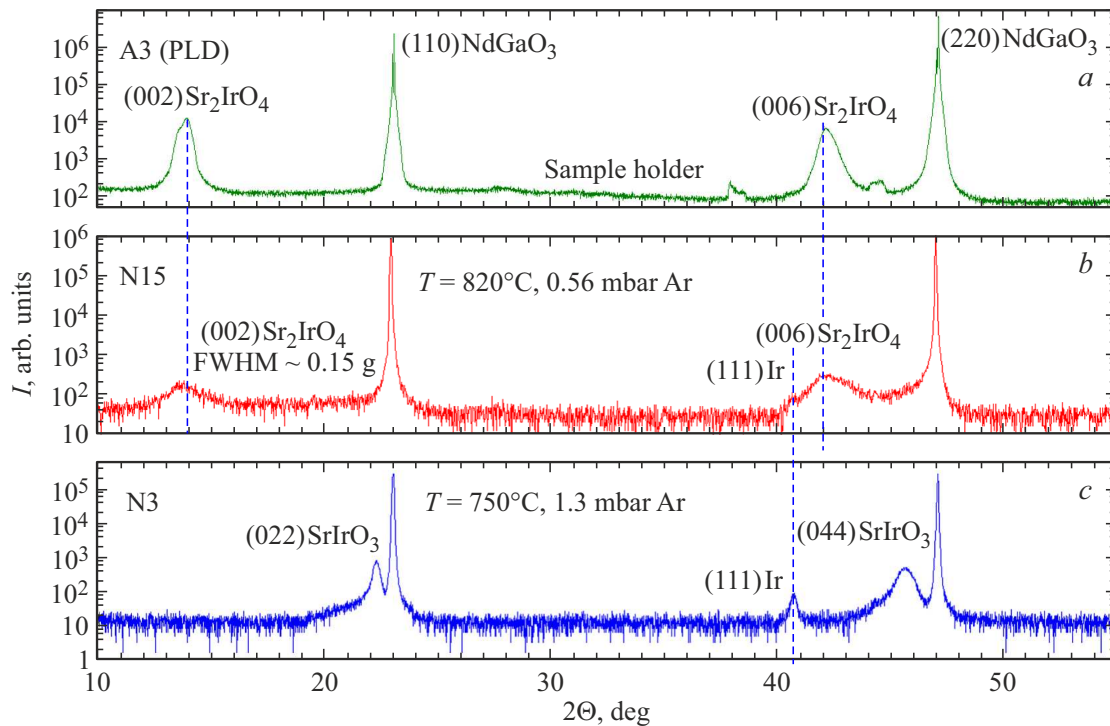
Figure 1. X-ray diffraction pattern, $\theta/2\Theta$ scan for three samples. A3 (PLD) was produced by the laser ablation method, N 3 and 15 were produced by DC cathode sputtering method.
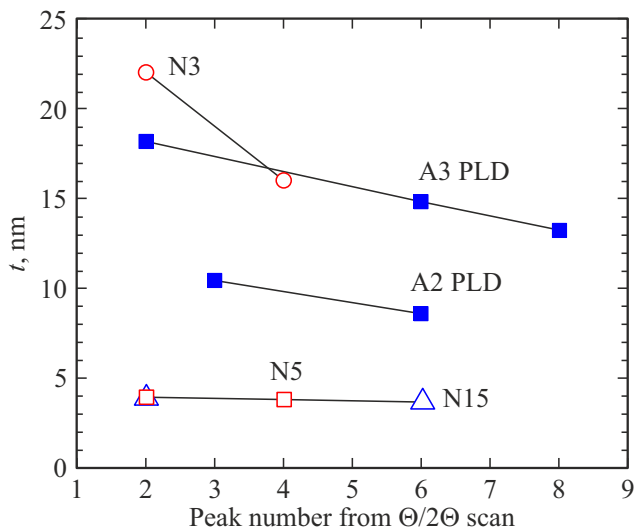
Figure 2. Film thicknesses calculated from the diffraction patterns. x axis is an X-ray peak number. y axis is the film thickness calculated from this peak. The lines connect the results for the same film, the are drawn by eye. Closed symbols are for the films produced by the PLD method, open symbols are for the films produced by the DC deposition method.

and when the rate was increased, a film with considerable content of polycrystalline iridium was produced.

For thin films, the main contribution in the peak full width at half maximum for X-ray diffraction pattern $\Delta(2\Theta)$ originates from the finite number of diffraction planes. Film thicknesses t are estimated from the diffraction pattern peak widths using the equation from [5]:

$$\frac{t}{\lambda} = \frac{1}{\Delta(2\Theta) \cdot \cos\Theta}, \tag{1}$$

where $\lambda = 0.154056$ nm is the X-ray wavelength. Film thicknesses calculated from the diffraction pattern peak widths are shown in Figure 2.

Film thicknesses obtained by the PLD method were known from the deposition rate calibration and film deposition time. Rate calibration was carried out by film deposition, etching a microbridge in it and measurement of the film thickness by a profilometer. Deposition rate calibration was not performed for films produced by the cathode deposition method, but thicknesses of these films were calculated from diffraction patterns. The data is shown in Figure 2. Calculation of thicknesses t by equation (1) gives the values which are true by the order of magnitude. Thus, for sample A3 PLD, the thickness determined by the calibrated rate was 34 nm, and the calculation from the diffraction pattern for peaks (002), (006), (008) gave $t = 8$, 15, 13 nm, respectively. For sample A2 PLD, the thickness determined from the calibrated rate was equal to 17 nm. The calculation gave $t = 11$ and 9 nm for peaks (003) and (006). Resistivities of films which were produced by DC sputtering were estimated using the calculated thicknesses.

3. Electrophysical properties

To compare the parameters of the films produced by the two deposition methods, Figure 3 shows the temperature dependences of resistance for two Sr_2IrO_4 samples.
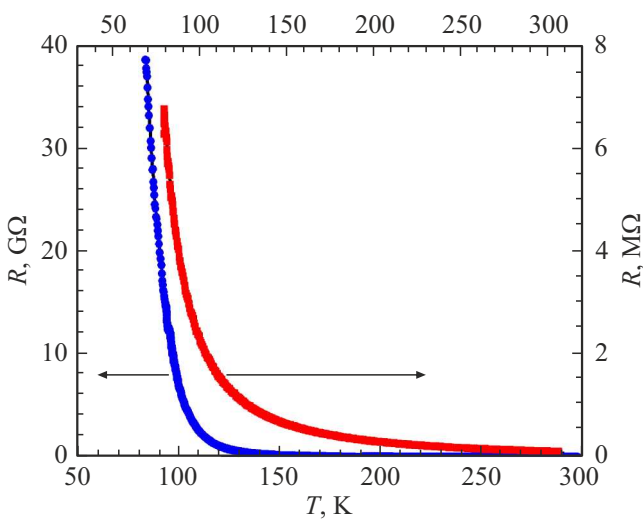
N 15 was produced by the DC-sputtering method at Ar pressure 0.5 mBar and $T = 820°C$, and A3 was obtained by the laser ablation method at Ar pressure 0.5 mBar and $T = 800-760°C$. Resistance of the sample produced by the PLD-sputtering method is much higher than that of the sample obtained by DC-sputtering. Since the substrates, to which thin films were deposited, were similar, the deposition method has the main effect on the electric transport properties. The temperature dependence of the resistivity of dielectric materials is described by thermal activation of the carriers model [6]:

$$\rho(T) = \rho_0 \exp\left(\frac{\Delta E}{2kT}\right), \qquad (2)$$
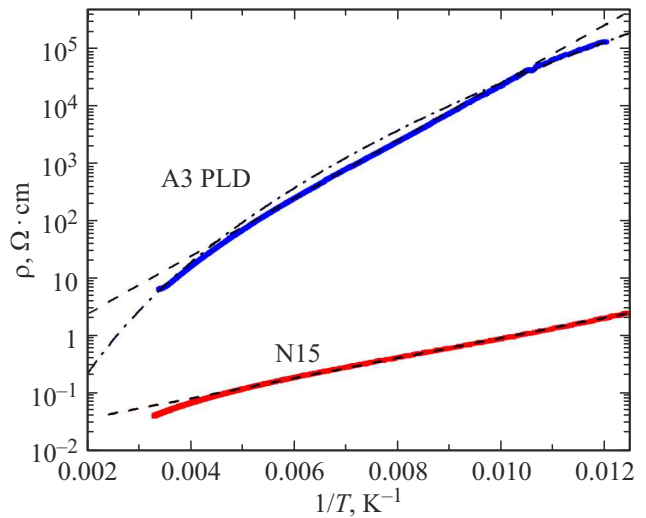
where $\rho(T)$ is the resistivity depending on temperature, ΔE is the activation energy, ρ_0 is the constant from the experiment, k is the Boltzmann constant, see Figure 4.

Approximations of the experimental dependences by equation (2) give $\Delta E \sim 200\,meV$ for laser deposited sample A3 PLD and $\Delta E \sim 70\,meV$ for DC-sputtered sample N 15.

Figure 5 shows the temperature dependences for $SrIrO_3$ films produced by the cathode sputtering method. The films differ depending on thickness; the same metal−insulator transition with decreasing film thickness was observed in [7]. For $t = 4\,nm$ film, N 5, activation dependence was obtained: $\rho(T) = 0.012 \cdot \exp(180/T)$ as shown in Figure 5, a. Resistivity of $t = 20\,nm$ film N 3 was about

Figure 4. Dependences of resistances on reciprocal temperature for Sr_2IrO_4 films. Sample A3 with thickness $t = 34\,nm$ was produced by PLD-sputtering, sample N 15 was produced by DC-sputtering, $t = 4\,nm$. Approximations of dependences according to the thermal activation of the carrier model — dashed lines, to three dimension hopping conductivity model — dashed-dotted line.

$0.2\,m\Omega \cdot cm$, therefore, a metallic conductivity mechanism was suggested for it, though the resistance grows a little with the decreasing temperature. For disordered metals, the conductivity may decrease with the decreasing temperature, for example, using the equation from [8]:

$$\sigma(T) = \sigma_0 + \sigma_T \cdot T^{1/2}, \qquad (3),$$

where the conductivity σ is a quantity inverse to resistivity, σ_0 and σ_T are constants obtained from the experiment. Approximation of the temperature dependence by equation (3) is shown in Figure 5, b.
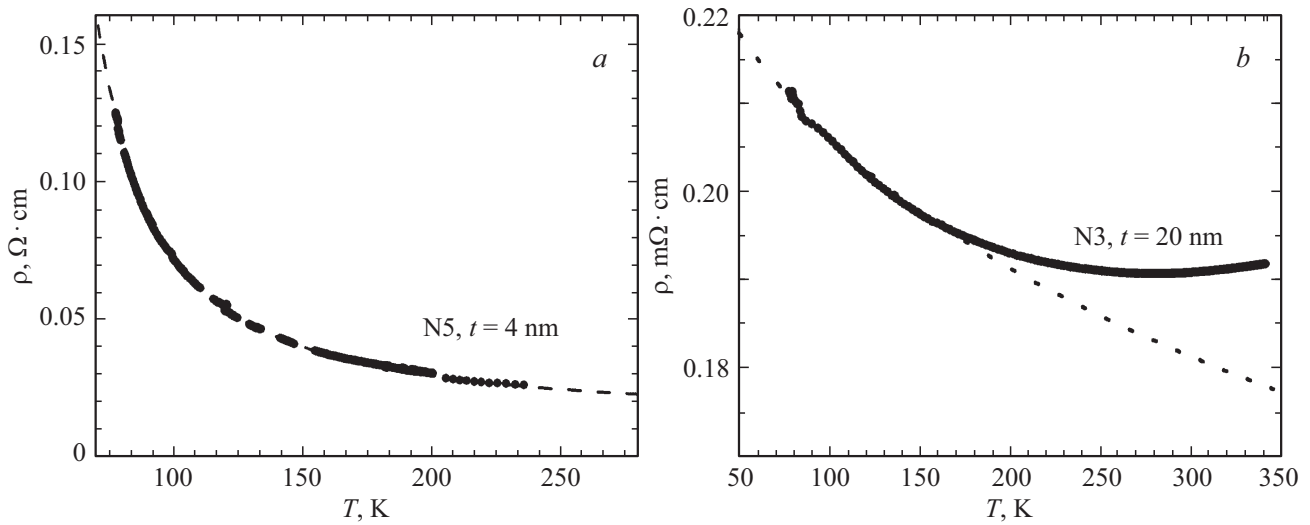
4. Results and discussion

For the discussion note that for dependence $\rho(T)$ for sample A3 PLD, a conductivity model with variable range hoping length is applicable (Figure 4):

$$\rho(T) = \rho_0 \exp\left(\frac{T_0}{T}\right)^{1/4}, \quad T_0 = \frac{24}{\pi k} \cdot \frac{1}{g\alpha^3}. \qquad (4)$$

Equation (4) was obtained in [9] with the following notations: $\rho(T)$ — resistivity depending on temperature, ρ_0 and T_0 — constants defined from the experiment, g — density of states at the Fermi level, α charge carrier radius at the impurity center.

Equation (4) was obtained in [9] with the following notations: $\rho(T)$ — resistivity depending on temperature, ρ_0 and T_0 — constants defined from the experiment, g — density of states at the Fermi level, α — a localization radius of a carrier at the impurity center. The experiment

Figure 3. Dependence of resistances on temperature for samples Sr_2IrO_4. Sample A3 PLD, $t = 34\,nm$, was deposited by the PLD method, data — blue dots, left and bottom scales. Sample N 15, $t = 4\,nm$, was produced by DC sputtering — red dots, right and top scales.

Figure 5. Dependences ρ on temperature for SrIrO$_3$ films. Figure 5, a shows the activation law approximation — dashed line. Figure 5, b shows approximation for disordered metal — dotted line. Thicknesses: N 5 — $t = 4$ nm, N 3 — $t = 20$ nm.

fitting as shown in Figure 4 gave $T_0 \sim 150 \cdot 10^6$ degrees Kelvin. In [4] the radius α in Sr$_2$IrO$_4$ was estimated as 0.5 nm, whence $g \sim 5 \cdot 10^{18}$ eV/cm^3 is derived. High resistances of laser films may be also explained by the tree-dimension hopping conductivity model with a variable range hoping length. The approximation of temperature dependences for laser films by this model gives high T_0 and low $\alpha \sim 0.5-1$ nm, which is close to the lattice cell sizes Sr$_2$IrO$_4$: A = 0.389 nm, C = 1.29 nm. Figure 4 shows that the activation model approximates the experimental curve for sample A3 PLD better that the hopping model in the temperature range $300-80$ K. To check whether the conductivity with a variable range hoping length is present in the temperature dependences of resistances, measurements at temperatures below 77 K are required.

For curve $\rho(T)$ for the DC-sputtered sample (Figure 4), the thermal activation model is suitable. $\Delta E \sim 70$ meV, which is lower than that of the PLD samples: $\Delta E \sim 200-260$ meV [10]. Alternative model: hopping conductivity to the nearest impurity centers at high impurity compensation is described in [11]. When the temperature dependence of resistance is written as

$$\rho(T) = \rho_3 \cdot \exp\left(\frac{\varepsilon_3}{kT}\right), \qquad (5)$$

where ε_3 is the energy of hop activation to the nearest impurity centers, ρ_3 is the pre-exponential factor depending on the temperature in a power-law manner. The dependence in the form of $\ln[\rho(T)] \sim 1/T$ will be observed for both mechanisms: mechanism of „hops to the adjacent centers" and activation mechanism. But the energy ε_3 is much lower than the band gap ΔE. The DC-sputtered film contains a polycrystalline iridium impurity which can be seen in the diffraction pattern in Figure 1, b. Iridium possibly creates impurity levels in the band gap and decreases the experimentally determined activation energy from ΔE to ε_3. The

theoretical band gap in Sr$_2$IrO$_4$ may reach ~ 620 meV [12], but for thin films, lower $\Delta E \sim 80-100$ meV are typical [6].

The temperature dependence of resistance of SrIrO$_3$ film with a low thickness of 4 nm shown in Figure 5, a is well approximated by the thermal activation model with $\Delta E \sim 30$ meV. The activation model is applicable, if $E > kT$ as shown in [13]. At 200 K, $kT \sim 17$ meV and this condition is satisfied. For approximation of dependence $\rho(T)$ of SrIrO$_3$ film with a higher thickness of $t = 20$ nm, Figure 5, b uses a disordered metal model and equation (3) from [8]. Resistivity of metals shall not exceed the Ioffe−Regel limit which is about 0.3 m$\Omega \cdot$ cm for alloys and about 10 m$\Omega \cdot$ cm for metals with electron−electron interaction [14]. Since the resistance of sample N 3 is below the Ioffe−Regel limit and grows with the decreasing temperature in a power-law manner, rather than in an exponential manner, this film is metallic.

5. Conclusion

The DC cathode sputtering method gives two sets of epitaxial films with compositions Sr$_2$IrO$_4$ and SrIrO$_3$, respectively. The process for production of such films is described. X-ray data and electrical and physical properties are described, the effect of thicknesses on the electrical and physical properties is shown, films produced by the cathode sputtering method and films produced by the laser ablation method are compared. Resistances of thin dielectric Sr$_2$IrO$_4$ films obtained by DC-sputtering are about three orders of magnitude lower than that of the films produced by the laser ablation. Lower resistances are possibly caused by the presence of doping impurities, e.g. metallic iridium, in the DC-sputtered iridate. X-ray diffraction patterns of these films produced by both processes show the presence of only one iridate phase: Sr$_2$IrO$_4$. Crystal lattice constants

for the films produced by both processes are almost the same. Thin $SrIrO_3$ films had metallic conductivity at average thicknesses, but, when the thickness was reduced to $t \sim 4\,\text{nm}$, activation-mechanism conductivity typical for dielectrics occurred in them.

Acknowledgments

Funding

Conflict of interest

The authors declare that they have no conflict of interest.

References

[1] K. Nishio, H.Y. Hwang, Y. Hikita. APL Mater. **4**, 036102 (2016).

[2] A. Gutierrez−Llorente, L. Iglesias, B. Rodrıguez−Gonzalez, F. Rivadulla. APL Mater. **6**, 091101 (2018).

[3] A.M. Petrzhik, K.Y. Constantinian, G.A. Ovsyannikov, A.V. Zaitsev, A.V. Shadrin, A.S. Grishin, Yu.V. Kislinskii, G. Cristiani, G. Logvenov. Phys. Rev. B **100**, 024501 (2019).

[4] A.M. Petrzhik, G. Cristiani, G. Logvenov, A.E. Pestun, N.V. Andreev, Yu.V. Kislinskii, G.A. Ovsyannikov. Tech. Phys. Lett. **43**, *6*, 554 (2017).

[5] J.P. Gong, M. Kawasaki, K. Fujito, R. Tsuchia, M. Yoshimoto, H. Koinuma. Phys. Rev. B **50**, 3280 (1994).

[6] C. Lu, A. Quindeau, H. Deniz, D. Preziosi, D. Hesse, M. Alex̄e. Appl. Phys. Lett. **105**, 082407 (2014).

[7] V. Fuentes, B. Vasic, Z. Konstantinovic, B. Martinez, L. Balcels, A. Pomar. J. Magn. Magn. Mater. **501**, 166419 (2020).

[8] M.E. Gershenzon, V.N. Gubankov, M.I. Falei. Sov. Phys. JETP **63**, *6*, 1287 (1986).

[9] N. Apsley, H.P. Hughes. Phil. Mag. **31**, 1327 (1975).

[10] Yu.V. Kislinskii, K.Y. Constantinian, I.E. Moskal, A.M. Petrzhik, A.V. Shadrin, G.A. Ovsyannikov. Phys. Solid State **64**, *10*, 1394 (2022).

[11] Boris I. Shklovski, Alex L. Efros. „Electronic properties of doped semiconductors." Springer Series in Solid-State Sciences. Book series SSSOL V. 45 (1984).

[12] Gang Cao, Pedro Schlottmann. Rep. Prog. Phys. **81**, 042502 (2018).

[13] K.-U. Barholz, M.Yu. Kupriyanov, U. Hubner, F. Schmidl, P. Seidel. Physica C **334**, 175 (2000).

[14] N.E. Hussey, K. Takenaka, H. Takagi. Phil. Mag. **84**, 2847 (2004).

Translated by Ego Translating